

# Multiphoton Absorption in Expanded Porphyrins

Yuanhang He<sup>1</sup>, Renjie Hui<sup>1</sup>, Yuanping Yi<sup>2</sup>, Zhigang Shuai<sup>2,\*</sup>

<sup>1</sup>School of Aerospace Science and Engineering, Beijing Institute of Technology, Beijing 100081, P. R. China;

<sup>2</sup>Institute of Chemistry, Chinese Academy of Sciences, Beijing 100080, P. R. China

**Abstract:** We have calculated the multiphoton absorption cross-sections for three expanded porphyrin derivatives using the sum-over-states-involved tensor approach in combination with the strongly correlated multireference determinant single- and double-configuration interaction method. The calculated results showed that the two- and three-photon energies corresponding to the first peak of the multiphoton absorption spectra showed a decrease (red-shifted) with the number of inserted thiophene groups, whereas the cross sections showed a remarkable increase, particularly for three-photon absorption cross-section. However, the larger twist of the molecular plane for the expanded molecule resulted in an obvious drop in the increasing trend for three-photon absorption cross-section.

**Key Words:** Multiphoton absorption; Sum-over-states-involved tensor approach; Porphyrin derivatives; Multireference determinant configuration interaction method

Multiphoton absorption (MPA) is a process in which an atom or molecule is excited from the ground state to the excited state by simultaneous absorption of two or more photons. Probing and designing of molecular materials with large MPA (particularly two- or three-photon absorption) cross-sections have attracted considerable interests from both theoretical and experimental standpoints due to their wide and potential applications in the fields of three-dimensional (3D) optical data storage, photodynamic therapy, and 3-D micro-fabrication<sup>[1–4]</sup>.

Many efforts have been devoted to the study of the dipolar, the quadrupolar, octupolar, and the multi-branched and dendritic molecules, which have been found to present relatively large MPA cross-sections<sup>[5–11]</sup>. It is shown that the origin of the large MPA cross-sections in these molecules is the effectively delocalized  $\pi$ -conjugated electrons.

Porphyrin derivatives, one of the most prominent MPA molecules, have attracted special attention because of their bio-compatibility, large conjugation plane, and the abundance of species<sup>[12–17]</sup>. However, little is known about the relationships between the molecular structures and their MPA properties, thereby requiring further systematic studies. In this work,

a quantum-chemical method as developed by the authors was applied to investigate three expanded porphyrins in order to gain deeper insights into understanding of the structure–property relationships for two- and three-photon absorptions.

## 1 Theoretical methods

The sum-over-states (SOS) method has been widely used for the computation of nonlinear optical (NLO) coefficients in organic molecules<sup>[18]</sup>. In this approach, the NLO coefficients of a molecule are directly expressed as summation over transition dipole moment products divided by transition energies. But it is a formidable task to calculate the high-order NLO coefficients, particularly the fifth-order NLO coefficients for three-photon absorption (3PA) *via* the full SOS approach, due to the huge amounts of computational costs involved. However, under the resonant conditions, the MPA cross-sections can also be obtained by the tensor approach, which still involves SOS, but with much less degree of summations.

In the tensor approach, the two- and three-photon absorption cross-sections are expressed by the transition matrix ele-

Received: October 24, 2007; Revised: December 21, 2007.

\*Corresponding author. Email: zgshuai@iccas.ac.cn; Tel: +8610-62521934; Fax: +8610-62525573.

The project was supported by the National Natural Science Foundation of China (10425420, 20433070).

Copyright © 2008, Chinese Chemical Society and College of Chemistry and Molecular Engineering, Peking University. Published by Elsevier BV. All rights reserved. Chinese edition available online at www.whxb.pku.edu.cn

ments  $S_{g \rightarrow f}^{ij}$  and  $T_{g \rightarrow f}^{ijk}$ , respectively, which is written as<sup>[12,19]</sup>,

$$S_{g \rightarrow f}^{ij} = \mathbf{P}_{ij} \sum_m \frac{\langle g | \bar{\mu}_i | m \rangle \langle m | \bar{\mu}_j | f \rangle}{E_{gm} - \hbar\omega - i\Gamma} \quad (1)$$

$$T_{g \rightarrow f}^{ijk} = \mathbf{P}_{ijk} \sum_{mn} \frac{\langle g | \bar{\mu}_i | m \rangle \langle m | \bar{\mu}_j | n \rangle \langle n | \bar{\mu}_k | f \rangle}{(E_{gm} - \hbar\omega - i\Gamma)(E_{gn} - 2\hbar\omega - i\Gamma)} \quad (2)$$

where  $i, j$ , and  $k$  denote the Cartesian coordinate ( $x, y, z$ ) of molecules;  $g$  represents the ground state;  $m, n$ , and  $f$  represent any states (including the ground state);  $E_{gm}$  is the transition energy from the ground state  $g$  to the excited state  $m$ ;  $\bar{\mu}_i$  is the  $i$ -component dipole displacement operator extracting the ground-state dipole moment; and  $\langle m | \bar{\mu}_i | n \rangle$  denotes the difference of state dipole moment between states  $m$  and  $g$  if  $m=n$ , otherwise it is the transition dipole moment between states  $m$  and  $n$ ;  $\hbar\omega$  is the input photon energy;  $\Gamma$  denotes the Lorentzian broadening factor; and  $\mathbf{P}_{ij}$  and  $\mathbf{P}_{ijk}$  are operators that sum over all terms generated by permutation over the indices  $i, j$ , and  $k$ . If the molecular orientations are averaged and if the isotropy is assumed, the two- and three-photon absorption cross-sections ( $\sigma_2$  and  $\sigma_3$ ) for linearly polarized input light can be expressed as<sup>[20]</sup>,

$$\sigma_2(\omega) = \frac{4\pi^2 L^4}{\hbar n^2 c^2} (\hbar\omega)^2 \sum_f \frac{1}{15} \left| \sum_{ij} [S_{g \rightarrow f}^{ii} (S_{g \rightarrow f}^{ij})^* + 2S_{g \rightarrow f}^{ij} (S_{g \rightarrow f}^{ij})^*] \right| \times \frac{\Gamma}{(E_{gf} - 2\hbar\omega)^2 + \Gamma^2} \quad (3)$$

$$\sigma_3(\omega) = \frac{4\pi^3 L^6}{3\hbar n^3 c^3} (\hbar\omega)^3 \sum_f \frac{1}{35} \left| \sum_{ijk} [2T_{g \rightarrow f}^{ijk} (T_{g \rightarrow f}^{ijk})^* + 3T_{g \rightarrow f}^{ijj} (T_{g \rightarrow f}^{kkj})^*] \right| \times \frac{\Gamma}{(E_{gf} - 3\hbar\omega)^2 + \Gamma^2} \quad (4)$$

where  $n$  is a refractive index (set to 1.0 in the vacuum),  $c$  is the speed of light in vacuum,  $\hbar$  is the Planck constant, and  $L=(n^2+2)/3$  denotes a local field correction. Similarly, the orientation-averaged one-photon absorption (1PA) cross-section is written as,

$$\sigma_1(\omega) = \frac{4\pi L^2}{\hbar n c} (\hbar\omega) \frac{2}{3} \sum_{im} \left| \langle g | \bar{\mu}_i | m \rangle \right|^2 \frac{\Gamma}{(E_{gm} - \hbar\omega)^2 + \Gamma^2} \quad (5)$$

In this article, the ground-state geometries of the molecules were optimized by density-functional theory with the hybrid Becke three-parameter Lee-Yang-Parr (B3LYP) functionals and the 6-31G\* basis set, as implemented in the Gaussian 03 package<sup>[21]</sup>. On the basis of the optimized geometries, the energies of the ground and excited states, as well as the transition dipole moments between these states were calculated by a multireference determinant configuration interaction using single- and double-excitations (MRDCI) method as fully implemented by the authors<sup>[22,23]</sup>, coupled with the semiempirical intermediate neglect of differential overlap (ZINDO) Hamiltonian<sup>[24]</sup>. The Mataga-Nishimoto potential was used to describe the Coulomb repulsion terms<sup>[25]</sup>. The selected reference determinants include the Hartree-Fock ground state, three singly excited configurations (HOMO→LUMO, HOMO−1→LUMO, and HOMO→LUMO+1), and one doubly excited

configuration (HOMO, HOMO→LUMO, LUMO). The active excitation space can include up to 15 occupied and 15 unoccupied orbitals, which amount to approximately  $3 \times 10^5$  configurations for a representative calculation, which is much larger than that the 6000 in original ZINDO program<sup>[25]</sup>. For the sake of consistency and computational feasibility, we selected all the continuous highest occupied  $\pi$  molecular orbitals (MOs) and the lowest unoccupied MOs to construct the configuration space<sup>[26]</sup>. For hexaphyrin molecule, the active space includes 8 occupied MOs and 11 virtual MOs; for relatively larger octaphyrin molecule, 11 occupied and 11 virtual active MOs were selected; the numbers of occupied and virtual active MOs reached 13, respectively, for the largest decaphyrin molecule. The Davidson iterative algorithm was used to diagonalize the Hamiltonian matrix, and approximately 130 singlet excited states were obtained to calculate the molecular MPA properties. Compared with the equation-of-motion coupled-cluster (EOM-CC) method<sup>[27]</sup>, MRDCI method contains higher order electron correlation effects, which is very important for properly describing the transition dipole moments between the excited states. Marder and Coe *et al.* have successfully applied our program to design two-photon absorbing molecular systems with large cross-sections<sup>[28–31]</sup>, and the experimental results were well rationalized by theoretical calculations with our codes.

It should be noted that the nonlinear response theory has achieved important progresses over the recent ten years, as represented by the successful implementation of the Dalton program package<sup>[32]</sup>. In fact, Shuai *et al.* also proposed a nonlinear response theory, called the correction vector (CV) method<sup>[25]</sup>, and have realized its computational program package in the frameworks of MRDCI and EOM-CC methods coupled with both *ab initio* and semiempirical model Hamiltonians<sup>[11]</sup>. The CV method is equivalent to the general nonlinear response theory for an exact ground state, but it is much simpler both in the formalism and in numerical computations. In principle, the response theory or CV method can give the MPA cross-sections directly from the ground-state properties. However, the convergence is not guaranteed for every input light frequency in the necessary iterative process for solving the linear equations, thus it is very difficult to obtain full electronic spectra, whereas the CV method has been shown to be always convergent. The drawback of the CV method is that the formalism is based on the exact ground state, but in practice we are always dealing with the approximate ground state. This would lead to certain inconsistency in the formulation. Despite all that, both numerical computations and theoretical expressions are much simpler for CV method than those for the response theory. It does not result in any principal problem if the ground state is well described. Nevertheless, for both response theory and CV method, they only provide numbers of MPA cross-sections at a given input frequency, which is not sufficient to provide a deep insight into

Table 1 Molecular ground-state geometries optimized by B3LYP/6-31G\* method

Molecule	hexaphyrin	octaphyrin	decaphyrin
Top view			
Side view			

the designs of the molecular materials with large MPA cross-sections. The SOS method as well as the tensor approach used in this work can provide more information on the structure–property relationships, for instance from the excited-state electronic structure and transition dipole-moment analysis, not just a number.

## 2 Results and discussion

The optimized ground-state geometries as well as the molecular  $xyz$  axes of the expanded porphyrins studied in this paper are presented in Table 1. With increasing the number of inserted thiophene rings, the  $\pi$  electrons become more delocalized. However, the molecular ring also becomes more and more twisted, leading to shorter effective  $\pi$ -electron conjugation.

The calculated one-photon absorption spectra for hexaphyrin, octaphyrin, and decaphyrin are shown in Fig.1. The absorption peaks are globally red-shifted as the molecular rings are expanded. For decaphyrin, the largest of the three, there are more features, partly due its more pronounced twist presented in the molecular plane. The experimental spectrum<sup>[15]</sup> for the fluorophenyl-substituted decaphyrin is also plotted in the inset of Fig.1(c) for the sake of comparison. The overall shape of the calculated spectrum shows good agreement with the spectrum measured in the experiment, although the ex-

perimental peak values are overestimated by a uniform value of approximately 0.3 eV. This is attributed to the larger steric hindrance due to the fluorophenyl groups in the real molecules, which has been simplified in simulation.

Over the spectral range below the first one-photon absorption, the 2PA spectra for the three molecules are shown in Fig.2. A similar red-shift can be observed as the molecular ring is enlarged from hexaphyrin to octaphyrin and then to decaphyrin. The 2PA peak for decaphyrin is approximately 0.74 eV. The calculated 2PA cross-sections are given in Table 2, where we also present an analysis on the “virtual” excitation channels from the transition dipole moments. From the most important channels contributing to the 2PA cross-section, we can find that the increment of  $\sigma_2$  from hexaphyrin to octaphyrin is mainly originated from the increase of transition dipole moments. There are a couple of reasons to rationalize a larger  $\sigma_2$  in decaphyrin than in octaphyrin: (i) the obvious increase in  $y$ -component transition dipole moments; (ii) smaller detuning energies for the  $xx$  transition channel; (iii) larger contribution from the  $xy$  transition channel (in which the components of transition dipole moments from the ground state to the intermediate state and then to the final state are along the  $x$ - and  $y$ -axis directions, respectively), see Table 2 for details.

Fig.3 shows the 3PA spectra for the three molecules in the

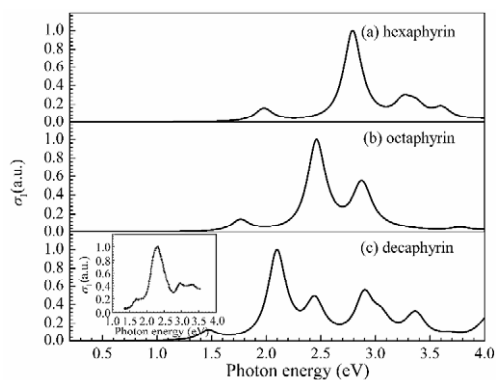


Fig.1 MRDCI/INDO calculated one-photon absorption spectra for the three molecules  
Experimental spectrum<sup>[15]</sup> was given in the inset of (c) for comparison.

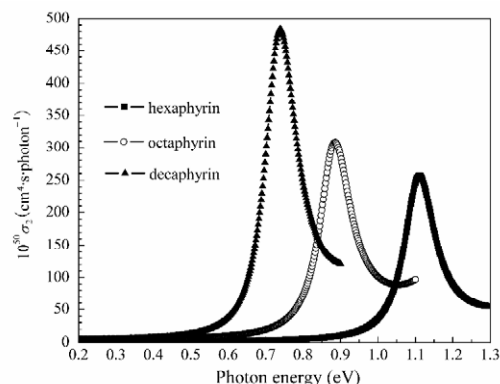


Fig.2 MRDCI/INDO calculated two-photon absorption spectra for the three molecules

Table 2 Two-photon energies ( $\hbar\omega$ ) and cross-sections ( $\sigma_2$ ) at the first peaks of the spectra for the three molecules, the dominant channels and their corresponding absolute values of the transition matrix elements

Molecule	$\hbar\omega/\text{eV}$	$10^{50}\sigma_2/(\text{cm}^4\cdot\text{s}\cdot\text{photon}^{-1})$	Channels <sup>a</sup>	$S$
hexaphyrin	1.11	257	$S_0 \xrightarrow[y]{7.87} S_2 \begin{pmatrix} 1.98 \\ 0.87 \end{pmatrix} \xrightarrow[y]{7.53} S_3 \begin{pmatrix} 2.21 \\ -0.01 \end{pmatrix}$	68.0
			$S_0 \xrightarrow[x]{17.15} S_5 \begin{pmatrix} 2.79 \\ 1.68 \end{pmatrix} \xrightarrow[x]{4.25} S_3 \begin{pmatrix} 2.21 \\ -0.01 \end{pmatrix}$	43.4
octaphyrin	0.89	308	$S_0 \xrightarrow[y]{-8.79} S_3 \begin{pmatrix} 1.76 \\ 0.87 \end{pmatrix} \xrightarrow[y]{7.76} S_2 \begin{pmatrix} 1.76 \\ -0.01 \end{pmatrix}$	77.4
			$S_0 \xrightarrow[x]{-20.51} S_5 \begin{pmatrix} 2.46 \\ 1.57 \end{pmatrix} \xrightarrow[x]{5.67} S_2 \begin{pmatrix} 1.76 \\ -0.01 \end{pmatrix}$	73.9
decaphyrin	0.74	483	$S_0 \xrightarrow[y]{17.27} S_3 \begin{pmatrix} 2.10 \\ 1.36 \end{pmatrix} \xrightarrow[y]{11.20} S_1 \begin{pmatrix} 1.47 \\ -0.01 \end{pmatrix}$	142.2
			$S_0 \xrightarrow[x]{-6.72} S_1 \begin{pmatrix} 1.47 \\ 0.73 \end{pmatrix} \xrightarrow[x]{-10.55} S_1 \begin{pmatrix} 1.47 \\ -0.01 \end{pmatrix}$	96.7
			$S_0 \xrightarrow[y]{17.27} S_3 \begin{pmatrix} 2.10 \\ 1.36 \end{pmatrix} \xrightarrow[x]{-7.03} S_2 \begin{pmatrix} 1.48 \\ 0.00 \end{pmatrix}$	89.2

<sup>a</sup>The value below the arrow line is the transition dipole moment or difference of state dipole moment (in  $10^{-30}$  C·m); index  $x$ ,  $y$ , or  $z$  above the arrow line denotes the direction of the dipole moment; the two values in parentheses represent the excitation energy (up) and the detuning energy (down), both expressed in eV.

spectral range for which the molecules are transparent for both one- and two-photon absorptions. Similar to the 2PA spectra, the 3PA spectra are also characterized by a single peak, and the 3PA photon energy at the peak is red-shifted, whereas the corresponding  $\sigma_3$  value shows an obvious increase as the ring is enlarged. From Tables 2 and 3, the increment of  $\sigma_3$  from hexaphyrin to octaphyrin or decaphyrin is more apparent with respect to that of  $\sigma_2$ , but when averaged by the number of inserted thiophene groups, the relative enhancement for 3PA is smaller. That is, the increasing trend for  $\sigma_3$  arising from the expanded molecular ring becomes less remarkable than that for  $\sigma_2$ . From the three important transition channels (which make the largest contributions to the 3PA peaks, see Table 3), we can find that the channels for hexaphyrin and octaphyrin are of identical types, namely, containing two  $xyx$  channels (the components of the three transition dipole moments from

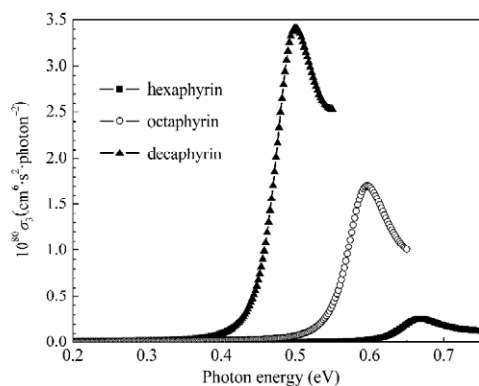


Fig.3 MRDCI/INDO calculated three-photon absorption spectra for the three molecules

the ground state to the first intermediate state to the second intermediate state and then to the final state are along molecular  $x$ ,  $x$ , and  $y$  axes, respectively) and one  $yyy$  component. Compared with hexaphyrin, octaphyrin possesses larger transition dipole moments and smaller detuning energies, which results in 6-fold increase in the  $\sigma_3$  value compared with octaphyrin. For decaphyrin, the most important channels are changed because as the number of inserted thiophene ring increases, the contribution along the  $y$  direction as well as the molecular plane twist also increases.

Fig.4 shows the evolution of the MPA cross-sections of the three molecules with respect to the number of intermediate states involved in summation. The three molecules present

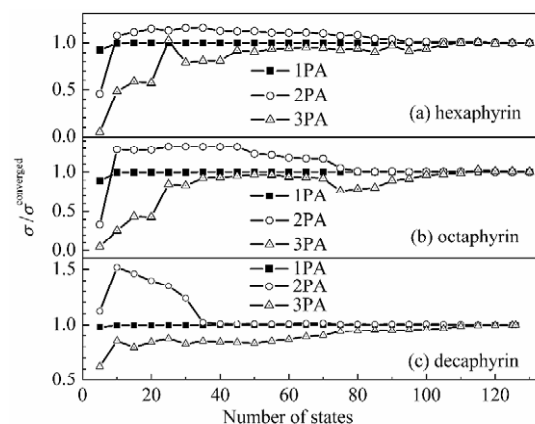


Fig.4 Evolution of one-, two-, and three-photon absorption cross-sections for the first peaks of the spectra for the three molecules with the number of intermediate states involved in summation in the tensor approach

Table 3 Three-photon energies ( $\hbar\omega$ ) and cross-sections ( $\sigma_3$ ) for the first peaks of the spectra for the three molecules, the dominant channels and their corresponding absolute values of the transition matrix elements

Molecule	$\hbar\omega/\text{eV}$	$10^{80}\sigma_3/(\text{cm}^6\cdot\text{s}^2\cdot\text{photon}^{-2})$	Channels	$T$
hexaphyrin	0.67	0.26	$S_0 \xrightarrow{x} S_5 \begin{pmatrix} 2.79 \\ 2.12 \end{pmatrix} \xrightarrow{x} S_0 \begin{pmatrix} 0.00 \\ -1.34 \end{pmatrix} \xrightarrow{y} S_2 \begin{pmatrix} 1.98 \\ -0.03 \end{pmatrix}$	813.6
			$S_0 \xrightarrow{y} S_2 \begin{pmatrix} 1.98 \\ 1.31 \end{pmatrix} \xrightarrow{y} S_3 \begin{pmatrix} 2.21 \\ 0.88 \end{pmatrix} \xrightarrow{y} S_2 \begin{pmatrix} 1.98 \\ -0.03 \end{pmatrix}$	385.7
			$S_0 \xrightarrow{x} S_5 \begin{pmatrix} 2.79 \\ 2.12 \end{pmatrix} \xrightarrow{x} S_3 \begin{pmatrix} 2.21 \\ 0.88 \end{pmatrix} \xrightarrow{y} S_2 \begin{pmatrix} 1.98 \\ -0.03 \end{pmatrix}$	293.4
octaphyrin	0.60	1.70	$S_0 \xrightarrow{x} S_5 \begin{pmatrix} 2.46 \\ 1.86 \end{pmatrix} \xrightarrow{x} S_0 \begin{pmatrix} 0.00 \\ -1.20 \end{pmatrix} \xrightarrow{y} S_3 \begin{pmatrix} 1.76 \\ -0.03 \end{pmatrix}$	1653.7
			$S_0 \xrightarrow{x} S_5 \begin{pmatrix} 2.46 \\ 1.86 \end{pmatrix} \xrightarrow{x} S_2 \begin{pmatrix} 1.76 \\ 0.56 \end{pmatrix} \xrightarrow{y} S_3 \begin{pmatrix} 1.76 \\ -0.03 \end{pmatrix}$	847.1
			$S_0 \xrightarrow{y} S_3 \begin{pmatrix} 1.76 \\ 1.16 \end{pmatrix} \xrightarrow{y} S_2 \begin{pmatrix} 1.76 \\ 0.56 \end{pmatrix} \xrightarrow{y} S_3 \begin{pmatrix} 1.76 \\ -0.03 \end{pmatrix}$	791.9
decaphyrin	0.50	3.41	$S_0 \xrightarrow{y} S_3 \begin{pmatrix} 2.10 \\ 1.60 \end{pmatrix} \xrightarrow{y} S_1 \begin{pmatrix} 1.47 \\ 0.47 \end{pmatrix} \xrightarrow{x} S_1 \begin{pmatrix} 1.47 \\ -0.04 \end{pmatrix}$	2686.9
			$S_0 \xrightarrow{x} S_1 \begin{pmatrix} 1.47 \\ 0.97 \end{pmatrix} \xrightarrow{x} S_1 \begin{pmatrix} 1.47 \\ 0.47 \end{pmatrix} \xrightarrow{x} S_1 \begin{pmatrix} 1.47 \\ -0.04 \end{pmatrix}$	1622.6
			$S_0 \xrightarrow{y} S_3 \begin{pmatrix} 2.10 \\ 1.60 \end{pmatrix} \xrightarrow{y} S_0 \begin{pmatrix} 0.00 \\ -1.00 \end{pmatrix} \xrightarrow{x} S_1 \begin{pmatrix} 1.47 \\ -0.04 \end{pmatrix}$	1247.9

similar evolutionary process.  $\sigma_1$  shows convergence within a few states. When tens of states are involved in the summation,  $\sigma_2$  is overestimated, and then it starts to decrease when more intermediate states are included, until convergence occurs. However,  $\sigma_3$  shows convergence until more than 100 intermediate states are included. In short, to obtain the converged values of higher order NLO coefficients using such SOS-involved method, more excited states are required.

### 3 Conclusions

We have performed calculations on three expanded porphyrins to investigate their multiphoton absorption properties using the tensor approach coupled with our MRDCI program. The calculated results show that the expansion of the molecular ring leads to a red shift for one- and multi-photon absorption spectra and a remarkable increase of two- and three-photon absorption cross-sections. The underlying mechanism involves detailed analysis based on molecular transition dipole-moments and energy detuning factors. These theoretical calculations can be helpful in the rational design of chromophores with large multiphoton absorption cross-sections.

### References

- Dvornikov, A. S.; Rentzepis, P. M. *Opt. Commun.*, **1995**, **119**: 341
- Fisher, W. G.; Partridge, W. P.; Dees, C.; Wachter, E. A. *Photochem. Photobiol.*, **1997**, **66**: 141
- Cumpston, B. H.; Ananthavel, S. P.; Barlow, S.; Dyer, D. L.; Ehrlich, J. E.; Erskine, L. L.; Heikal, A. A.; Kuebler, S. M.; Lee, I. Y. S.; McCord-Maughon, D.; Qin, J. Q.; Rockel, H.; Rumi, M.; Wu, X. L.; Marder, S. R.; Perry, J. W. *Nature*, **1999**, **398**: 51
- He, G. S.; Markowicz, P. P.; Lin, T. C.; Prasad, P. N. *Nature*, **2002**, **415**: 767
- Pati, S. K.; Marks, T. J.; Ratner, M. A. *J. Am. Chem. Soc.*, **2001**, **123**: 7287
- Rumi, M.; Ehrlich, J. E.; Heikal, A. A.; Perry, J. W.; Barlow, S.; Hu, Z. Y.; McCord-Maughon, D.; Parker, T. C.; Rockel, H.; Thayumanavan, S.; Marder, S. R.; Beljonne, D.; Bredas, J. L. *J. Am. Chem. Soc.*, **2000**, **122**: 9500
- Beljonne, D.; Wenseleers, W.; Zojer, E.; Shuai, Z. G.; Vogel, H.; Pond, S. J. K.; Perry, J. W.; Marder, S. R.; Bredas, J. L. *Adv. Funct. Mater.*, **2002**, **12**: 631
- Drobizhev, M.; Karotki, A.; Dzenis, Y.; Rebane, A.; Suo, Z. Y.; Spangler, C. W. *J. Phys. Chem. B*, **2003**, **107**: 7540
- Drobizhev, M.; Karotki, A.; Kruk, M.; Dzenis, Y.; Rebane, A.; Suo, Z.; Spangler, C. W. *J. Phys. Chem. B*, **2004**, **108**: 4221
- Zhu, L. Y.; Yi, Y. P.; Shuai, Z. G.; Bredas, J. L.; Beljonne, D.; Zojer, E. *J. Chem. Phys.*, **2006**, **125**: 044101
- Yi, Y.; Li, Q.; Zhu, L.; Shuai, Z. *J. Phys. Chem. A*, **2007**, **111**: 9291
- Zhu, L. Y.; Yang, X.; Yi, Y. P.; Xuan, P. F.; Shuai, Z. G.; Chen, D. Z.; Zojer, E.; Bredas, J. L.; Beljonne, D. *J. Chem. Phys.*, **2004**, **121**: 11060
- Zhu, L. Y.; Yi, Y. P.; Shuai, Z. G.; Schmidt, K.; Zojer, E. *J. Phys.*

- Chem. A*, **2007**, **111**: 8509
- 14 Rath, H.; Sankar, J.; PrabhuRaja, V.; Chandrashekar, T. K.; Nag, A.; Goswami, D. *J. Am. Chem. Soc.*, **2005**, **127**: 11608
- 15 Rath, H.; Prabhuraja, V.; Chandrashekar, T. K.; Nag, A.; Goswami, D.; Joshi, B. S. *Org. Lett.*, **2006**, **8**: 2325
- 16 Ahn, T. K.; Kwon, J. H.; Kim, D. Y.; Cho, D. W.; Jeong, D. H.; Kim, S. K.; Suzuki, M.; Shimizu, S.; Osuka, A.; Kim, D. *J. Am. Chem. Soc.*, **2005**, **127**: 12856
- 17 Ahn, T. K.; Kim, K. S.; Kim, D. Y.; Noh, S. B.; Aratani, N.; Ikeda, C.; Osuka, A.; Kim, D. *J. Am. Chem. Soc.*, **2006**, **128**: 1700
- 18 Orr, B. J.; Ward, J. F. *Mol. Phys.*, **1971**, **20**: 513
- 19 Cronstrand, P.; Luo, Y.; Norman, P.; Agren, H. *Chem. Phys. Lett.*, **2003**, **375**: 233
- 20 McClain, W. M. *J. Chem. Phys.*, **1971**, **55**: 2789
- 21 Frisch, M. J.; Trucks, G. W.; Schlegel, H. B.; et al. Gaussian 03, Revision B.05. Pittsburgh PA: Gaussian Inc., 2003
- 22 Buenker, R. J.; Peyerimhoff, S. D. *Theor. Chim. Acta*, **1974**, **35**: 33
- 23 Ridley, J.; Zerner, M. *Theor. Chim. Acta*, **1973**, **32**: 111
- 24 Mataga, N.; Nishimoto, K. *Z. Phys. Chem.*, **1957**, **12**: 35
- 25 Yi, Y. P.; Zhu, L. Y.; Shuai, Z. *J. Chem. Phys.*, **2006**, **125**: 164505
- 26 Albert, I. D. L.; Morley, J. O.; Pugh, D. *J. Chem. Phys.*, **1995**, **102**: 237
- 27 Zhu, L. Y.; Yi, Y. P.; Shuai, Z. *J. Mol. Sci.*, **2005**, **21**: 1
- 28 Chung, S. J.; Zheng, S. J.; Odani, T.; Beverina, L.; Fu, J.; Padhila, L. A.; Biesso, A.; Hales, J. M.; Zhan, X. W.; Schmidt, K.; Ye, A. J.; Zojer, E.; Barlow, S.; Hagan, D. J.; van Stryland, E. W.; Yi, Y. P.; Shuai, Z.; Pagani, G. A.; Brédas, J. L.; Perry, J. W.; Marder, S. R. *J. Am. Chem. Soc.*, **2006**, **128**: 14444
- 29 Coe, B. J.; Samoc, M.; Samoc, A.; Zhu, L. Y.; Yi, Y. P.; Shuai, Z. *J. Phys. Chem. A*, **2007**, **111**: 472
- 30 Zheng, S. J.; Beverina, L.; Fu, J.; Padilha, L.; Zojer, E.; Barlow, S.; Fink, C.; Kwon, O.; Yi, Y. P.; Shuai, Z.; van Stryland, E. W.; Hagan, D. J.; Brédas, J. L.; Marder, S. R. *Chem. Commun.*, **2007**: 1372
- 31 Zheng, S. J.; Leclercq, A.; Fu, J.; Beverina, L.; Padilha, L.A.; Zojer, E.; Schmidt, K.; Barlow, S.; Luo, J. D.; Jen, A.; Yi, Y. P.; Shuai, Z.; van Stryland, E. W.; Hagan, D. J.; Brédas, J. L.; Marder, S. R. *Chem. Mater.*, **2007**, **19**: 432
- 32 Angeli, C.; Bak, K. L.; Bakken, V.; et al. Dalton, an *ab initio* electronic structure program. release 1.2, 2001. available from <http://www.kjemi.uio.no/software/dalton/dalton.html>.